

## Impedance Analysis for Four Types of Mineral Water and Aquades Using Electrical Impedance Spectroscopy (EIS) at Frequencies of 1 Hz - 50 kHz

Darmawati Wulandari<sup>1</sup>, Ahmad Zarkasi<sup>1\*</sup>, Kholis Nurhanafi<sup>1</sup>

<sup>1</sup> Physics Department, Faculty Mathematics and Natural Science University of Mulawarman, Samarinda, Indonesia.

Corresponding Authors E-mail: [ahmad.zarkasi@fmipa.unmul.ac.id](mailto:ahmad.zarkasi@fmipa.unmul.ac.id)

---

### Article Info

#### Article info:

Received: 29-08-2023

Revised: 13-12-2023

Accepted: 15-12-2023

#### Keywords:

Mineral Water; Aquades; Warburg; Randles; EIS; Impedance

#### How To Cite:

D. Wulandari, A. Zarkasi, and K. Nurhanafi, "Impedance Analysis for Four Types of Mineral Water and Aquades Using Electrical Impedance Spectroscopy (EIS) at Frequencies of 1 Hz - 50 kHz", *Indonesian Physical Review*, vol. 7, no. 1, p 84-94, 2024.

#### DOI:

<https://doi.org/10.29303/ipr.v7i1.269>

### Abstract

The Electrical Impedance Spectroscopy (EIS) method can be used to identify minerals in mineral water. The EIS method measures the impedance of a material by injecting alternating current in a certain frequency range, which is non-invasive and non-destructive. This study aims to analyze the impedance of mineral water and aquades based on the influence of the dissolved content using EIS equipment that provides flexibility in adjusting the desired frequency spectrum. The study used a frequency range from 1 Hz to 50 kHz with a four-electrode configuration. The measurement graph results were analyzed using Bode graph with impedance plot and phase shift angle to determine the impedance characteristics of mineral water. Equivalent circuit modeling helped to identify the electrochemical properties of materials such as the Warburg circuit, Constant Phase Element (CPE), and Randles circuit. The results show that the aquades has a higher impedance compared to the four mineral waters. Additionally, the four mineral waters exhibit varying impedances, attributed to their respective mineral content. Mineral water is characterized by an impedance that is dominated by Warburg impedance ( $Z_w$ ) at low frequencies, charge transfer resistance ( $R_{ct}$ ) and double layer capacitance ( $C_{dl}$ ) at middle frequencies, and electrolyte resistance at high frequencies. However, the impedance of aquades dominated by electrolyte resistance ( $R_e$ ) at low frequency and  $R_e+R_{ct}$  at high frequency.

Copyright © 2024 Authors. All rights reserved.

### Introduction

Mineral water is one of the main sources of water consumed by humans [1], [2]. Natural mineral water comes from underground reservoirs [3]-[6], springs with one or more natural sources [2] or drilled sources containing a combination of major cations [7], [8] and certain compounds in varying amounts depending on the source [9]. Mineral water is a rich source of copper, zinc, iron, magnesium, fluorine, sodium and calcium [10], [11]. Mineral water is basically water that can be directly consumed without further processing such as distillation

or deionization [6]. The minerals contained in mineral water can be identified by analyzing the electrical conductivity of mineral water, which is influenced by the cations and anions contained in it. Electrical impedance and electrical conductivity are interrelated electrical properties [12]. Impedance is defined as resistance in an Alternating Current (AC) circuit and is expressed in units of Ohm ( $\Omega$ ) [13]. Measurement of the impedance of a material can use the EIS method.

EIS is a method to measure the relationship between current and potential difference including resistance, capacitance and inductance applied in the frequency domain [14], [15]. The EIS method is carried out to decipher the ohmic resistance and frequency-dependent resistance, namely impedance [16], the frequency helps identify the contribution of influential components in the mineral water and the interaction between the electrode and the electrolyte. EIS is done by injecting alternating current [17] with a small amplitude as input and then measuring the potential as the resulting response [18]. The advantages of the EIS method in characterizing the impedance of materials [14], [19]-[21] are non-invasive [22]-[25], non-destructive [26]-[28], and low cost [15], [29]. Until now, there are still many studies that analyze between electrolyte content and electrical impedance values such as impedance measurements in NaCl solution with the effect of concentration which is known that the higher the NaCl concentration, the impedance decreases [12]. Therefore, this study aims to determine the impedance comparison of aquades and four types of mineral water which of course have different characteristics and based on the minerals contained in it.

### Experimental Method

The materials tested in this study are four different mineral water samples and aquades. Signal generator AD9833 will provide an AC voltage of 0.627 A with a certain frequency then connected to a VCCS. VCCS (Voltage-Controlled Current Sources) is a circuit that produces current in response to a given voltage with the same frequency value as the input. The output alternating current from the VCCS is injected into the material through a copper electrode plate with a frequency range of 1 Hz - 50 kHz. Testing in the frequency range of 1 Hz - 55kHz is done because in that range VCCS and Signal Generator can work well and output the same voltage and frequency. Material testing was carried out in a cube-shaped chamber container measuring 2.5 cm long, 2.5 cm wide and 3 cm high using electrode plates measuring 0.5 cm wide and 2 cm high with a four-electrode configuration. The measurement results will be seen on the oscilloscope display in the form of sinusoidal signals, so that the output voltage and phase shift angle can be known.

Based on the results of the output voltage measurement, the impedance ( $Z$ ) will be calculated using equation (1) which is a decrease from Ohm's Law [30]:

$$Z = \frac{V}{I} \quad (1)$$

From the equation, it is known that  $V$  is the voltage out of the measured material and  $I$  is the current injected into the material. It is known that  $V$  and  $I$  are phasors that take into account the amplitude and phase of the sinusoidal signal function. To find out the size of the phase shift angle, it is calculated from the peak-to-peak distance between the input signal, namely the current signal ( $I$ ) and the output signal, namely the voltage signal ( $V$ ).

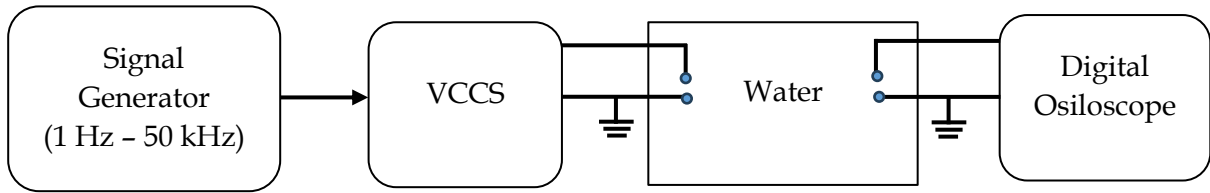


Figure 1. Block diagram of device design

### Result and Discussion

The input and output signals generated from the mineral water test can be seen in Figure 1, where the yellow signal is the input signal and the green signal is the output signal of the tested mineral water. The impedance test results of mineral water show that at low frequencies there is a second phase shift between the input signal and the output signal as shown in Figure 1, while at high frequencies the input and output signals do not experience a phase shift as seen in Figure 2.

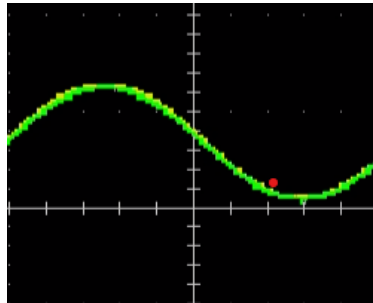


Figure 1. In-Phase Input and Output Signals

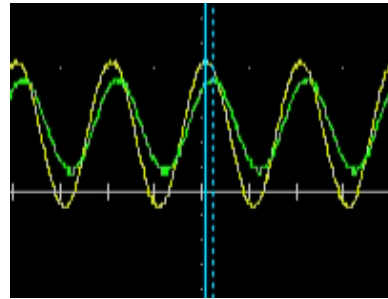


Figure 2. Input and Output signals with Phase difference

The results of impedance measurements on the four mineral water samples and aquades using current injection through parallel electrode plates are shown in Figure 3 for impedance and Figure 4 for phase shift angle presented with Bode plots. Bode plot is a frequency domain method where the x-axis is the log frequency and the y-axis is the measured impedance value or phase angle. Bode plots are widely used for the analysis of impedance-based systems. [31], [32]. Based on the graph, it is known that there are several influences on the decrease in impedance, namely the magnitude of the frequency value and the content in the solution. The impedance of aquades is greater than the four sample mineral water samples, this is due to aquades which has very little ion content. The impedance of mineral water and aquades decreases as the frequency value increases. The smaller the frequency, the greater the measured impedance, otherwise the greater the frequency, the smaller the measured frequency.

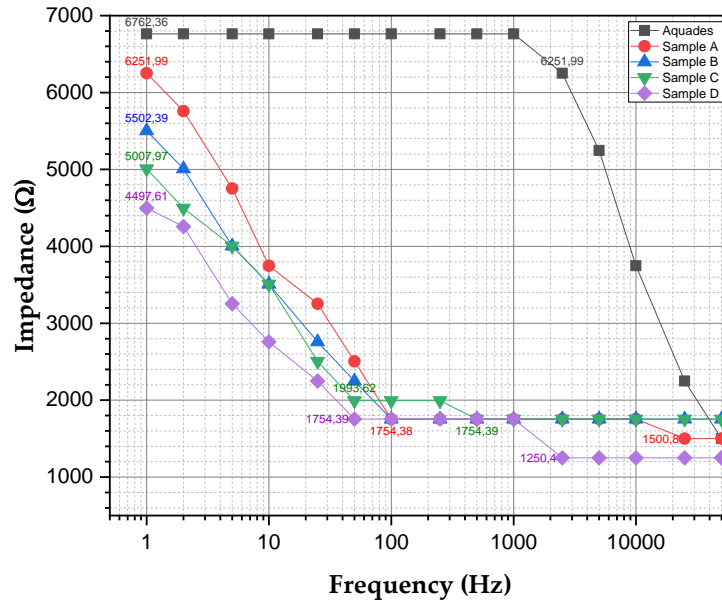


Figure 3. Impedance graph of aquades and four mineral water samples

The phase shift angle in mineral water with aquades is different as seen in Figure 4. The phase shift in aquades tends to increase at a frequency of 1 kHz - 50kHz, whereas in mineral water the phase shift will decrease in the frequency range of 1 kHz - 50kHz. This can indicate that the phase shift angle of  $0^\circ$  the solution is resistive, otherwise if there is a change in phase shift then the solution is capacitive. Therefore, it can be seen that aquades is more resistive than mineral water.

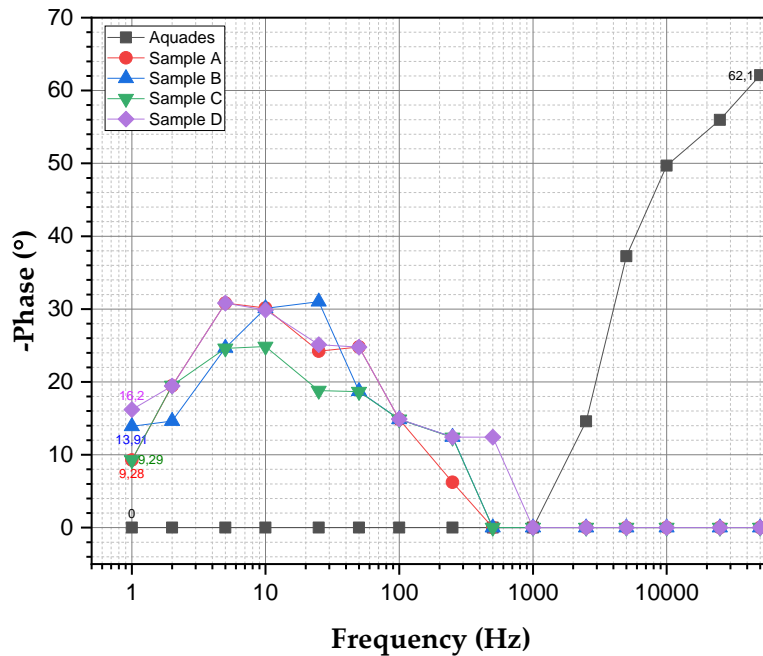


Figure 4. Phase shift angle graphs of aquades and four mineral water samples

Equivalent circuits are usually used to model the impedance properties or characteristics of a material [32] shown in Figure 5, or commonly known as the Randles circuit. Where  $R_e$  is the pure ohmic resistance of the solution  $R_{ct}$  is the electrode charge transfer resistance and  $C_{dl}$  is the double layer capacitance [33].  $R_{ct}$  is formed due to the redox reaction of the solution with the electrode which depends on the charge transfer, charge transfer rate, content in the solution.  $C_{dl}$  is formed at the electrode interface due to the potential difference between the electrode and the electrolyte [27], [33].  $R_e$  is the pure electrical resistance of the solution which is influenced by the characteristics and properties of the material being tested [34], [35].

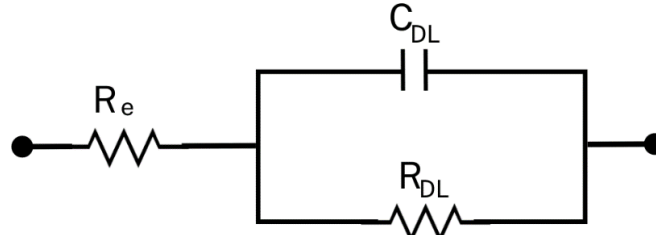


Figure 5. Randles Circuit

A series of Randles circuits can be used to model the impedance of aquades. It can be seen in Figure 6, in the frequency range of 1 Hz - 1000 Hz the impedance of aquades is resistive and above the frequency range of 1000 Hz the impedance in aquades is capacitive. At low frequencies the capacitor component in the Randles circuit will experience a slower discharge and can be analogized as a disconnected cable so that the electric current will go through  $R_{dl}$ , so that the total impedance is the sum of  $R_e$  and  $R_{dl}$ , otherwise at high frequencies the capacitor will experience a fast discharge before the capacitor is fully charged which results in a smaller capacitor capability analogous to a connected cable so that the electric current will go through the capacitor rather than through the resistor so that the impedance decreases but the phase shift angle increases. However, the Randles circuit can be modified to adjust the impedance measurement results of a material because each material has different characteristics.

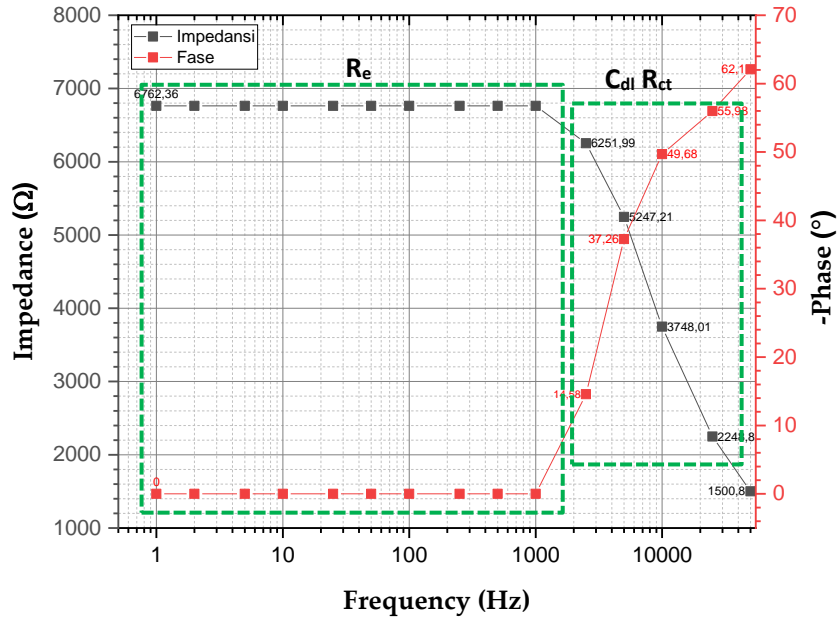


Figure 6. Impedance graph and phase shift angle of Aquades

Based on these characteristics, the Randles circuit is modified to model the results of impedance measurements on mineral water samples due to the inhomogeneity of the surface at the electrode interface so that the  $C_{dl}$  component in the Randles circuit is converted into a constant phase element (CPE) to assist in the analysis of measurement graphs and better compensate for the behavior of non-ideal capacitors [22], [36], [37] and there is an additional Warburg impedance component ( $Z_w$ ) that occurs at low frequencies of 1 Hz - 2 Hz caused by the diffusion phenomenon between ions and mineral water molecules with electrodes as shown in Figure 7.

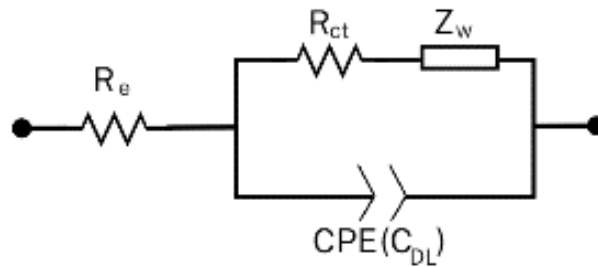
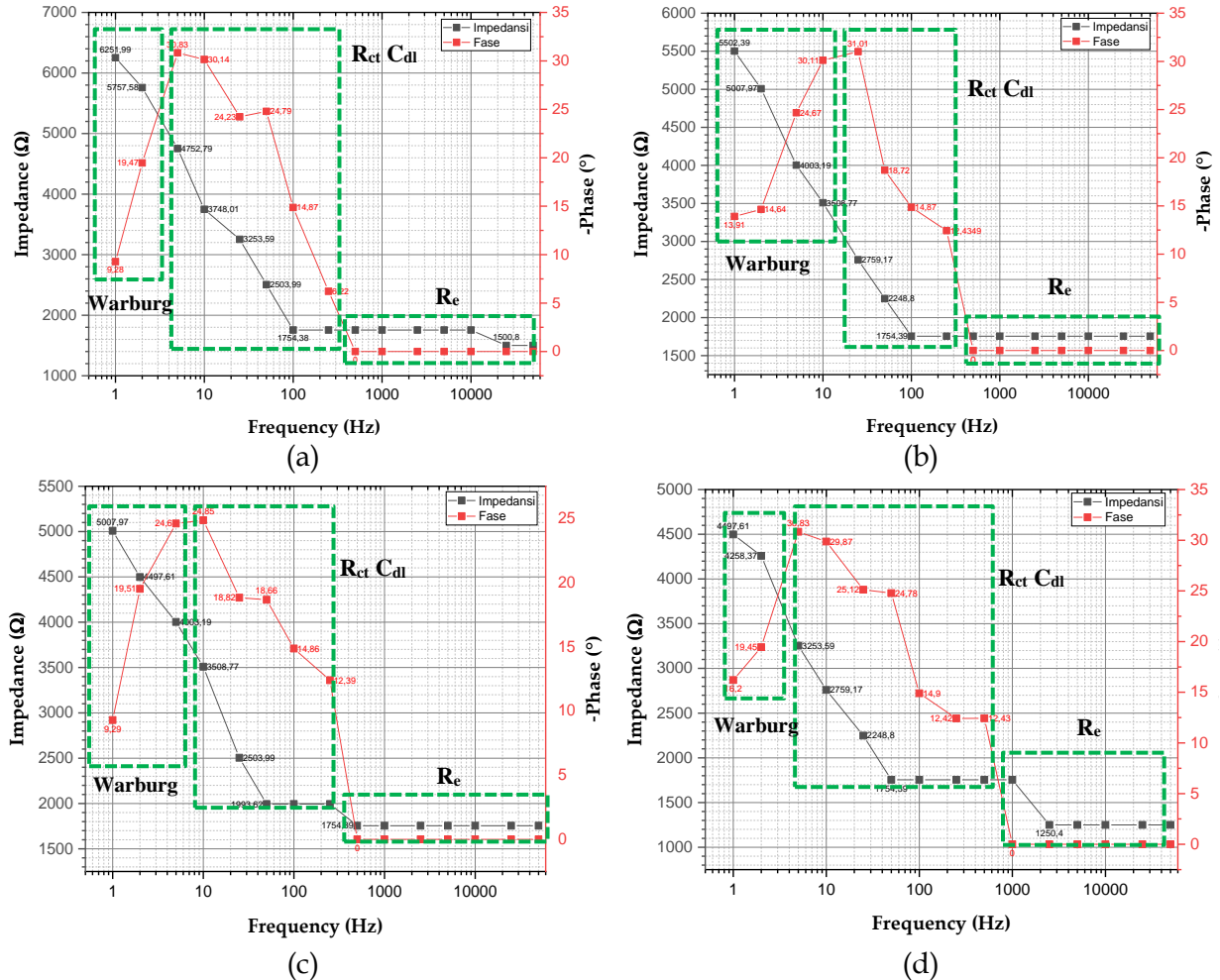


Figure 7. Modification of Randles Circuit

Impedance of mineral water has different characteristics from aquades. This is due to some mineral water content such as copper, zinc, iron and other chemical content [10] whose amount will affect the impedance measurement results as seen in Figure 8(a) for mineral water sample A. Impedance in mineral water has different characteristics that we can divide into three parts based on the phase shift. At low frequencies of 1 Hz - 2 Hz the impedance decreases while the phase shift angle increases, the intermediate frequency of 2 Hz - 250 Hz the impedance decreases and the phase shift angle also decreases and in the high frequency range of 500 Hz - 50 kHz the impedance decreases and the constant phase shift angle is  $0^\circ$ .



**Figure 8.** Impedance graph and phase shift angle of mineral water (a) Sample A, (b) Sample B, (c) Sample C, (d) Sample D

Mineral water that has impedance from highest to lowest in order is sample A which is 6251.99 Ω seen in Figure 8(a), sample B which is 5502.39 Ω seen in Figure 8(b), sample C which is 5007.97 Ω seen in Figure 8(c), and sample D which is 4497.61 Ω seen in Figure 8(d). This impedance difference can indicate the amount of content in the mineral water. The more the amount of solute content in mineral water, the smaller the measured impedance will be.

The impedance characteristics of the four mineral water samples are almost the same, which are divided into three parts based on the phase shift angle with its equivalent circuit components of  $R_e$ ,  $R_{ct}$ , CPE and Warburg Impedance ( $Z_w$ ). Sample D has a more dominant CPE impedance and has the lowest total impedance compared to aquades and the other three mineral water samples. This low impedance can occur because the content of ions, molecules or solutes in it is more than other solutions.

### Conclusion

The impedance of distilled water and the four mineral water samples injected with alternating current in the frequency range of 1 Hz - 50 kHz is different. Aquades has the highest impedance of 6762.36 Ω because aquades has very little ion content compared to mineral

water. The higher the content of ions, molecules and solutes in mineral water, the smaller the total impedance measurement results. The highest to lowest impedance of the four mineral waters in sequence is mineral water A of 6251.99  $\Omega$ , sample B of 5502.39  $\Omega$ , sample C of 5007.97  $\Omega$ , and sample D of 4497.61  $\Omega$ . In each mineral water there are changes in impedance characteristics that are different, it is influenced by the composition, non-homogeneity, double layer effect and interaction between electrodes and electrolyte. The measured impedance properties are differentiated based on the phase difference, namely constant Warburg impedance ( $Z_w$ ) constant phase element (CPE), electrolyte resistance (Re), charge transfer resistance (Rct).

### Acknowledgment

Thank to the supervisors and friends of the Electronics and Instrumentation Laboratory, Mulawarman University who have provided assistance and support to complete this research.

### References

- [1] N. D. Chau and B. Tomaszewska, *Mineral and Bottled Water as Natural Beverages*. Elsevier Inc., 2019. doi: 10.1016/b978-0-12-815272-0.00001-5.
- [2] C. Voica, G. Cristea, and I. Feher, *Multielement and Isotopic Characterization of Bottled Mineral Waters on the Romanian Market*. Elsevier Inc., 2019. doi: 10.1016/b978-0-12-815272-0.00005-2.
- [3] S. Quattrini, B. Pampaloni, and M. L. Brandi, "Natural mineral waters: chemical characteristic and health effects," *Hippel's Briefe von 1775 bis 1785*, vol. 13, no. 3, pp. 173–180, 2012, doi: 10.1515/9783110819700.306.
- [4] M. Guadayol, M. Cortina, J. M. Guadayol, and J. Caixach, "Determination of dimethyl selenide and dimethyl sulphide compounds causing off-flavours in bottled mineral waters," *Water Res.*, vol. 92, pp. 149–155, 2016, doi: 10.1016/j.watres.2016.01.016.
- [5] B. Jain, A. K. Singh, and M. A. B. H. Susan, *The World Around Bottled Water*. Elsevier Inc., 2019. doi: 10.1016/b978-0-12-815272-0.00002-7.
- [6] I. L. Bulia and J. Enzweiler, "The hydrogeochemistry of bottled mineral water in São Paulo state, Brazil," *J. Geochemical Explor.*, vol. 188, no. 2017, pp. 43–54, 2018, doi: 10.1016/j.gexplo.2018.01.007.
- [7] P. Dobosy, Á. Illés, A. Endrédi, and G. Záray, "Lithium concentration in tap water, bottled mineral water, and Danube River water in Hungary," *Sci. Rep.*, vol. 13, no. 1, p. 12543, 2023, doi: 10.1038/s41598-023-38864-6.
- [8] I. Chmielewska, S. Chalupnik, M. Wysocka, and A. Smolinski, "Radium measurements in bottled natural mineral-, spring- And medicinal waters from Poland," *Water Resour. Ind.*, vol. 24, no. June, 2020, doi: 10.1016/j.wri.2020.100133.
- [9] D. Di Giuseppe, "Comparison of the mineral element content of public drinking fountains and bottled water: A case study of Ferrara city," *Geosci.*, vol. 7, no. 3, 2017, doi: 10.3390/geosciences7030076.



- [10] R. Ranjbar, F. Khamesipour, N. Jonaidi-Jafari, and E. Rahimi, "Helicobacter pylori in bottled mineral water: Genotyping and antimicrobial resistance properties," *BMC Microbiol.*, vol. 16, no. 1, pp. 1–10, 2016, doi: 10.1186/s12866-016-0647-1.
- [11] E. Schnug, S. H. Haneklaus, U. Hundhausen, F. Knolle, F. Jacobs, and M. Birke, *Significance of Geographical, Hydrogeological, and Hydrogeochemical Origin for the Elemental Composition of Bottled German Mineral Waters*. Elsevier Inc., 2019. doi: 10.1016/b978-0-12-815272-0.00011-8.
- [12] C. S. Widodo, H. Sela, and D. R. Santosa, "The effect of NaCl concentration on the ionic NaCl solutions electrical impedance value using electrochemical impedance spectroscopy methods," *AIP Conf. Proc.*, vol. 2021, no. 2018, 2018, doi: 10.1063/1.5062753.
- [13] A. R. C. Bredar, A. L. Chown, A. R. Burton, and B. H. Farnum, "Electrochemical Impedance Spectroscopy of Metal Oxide Electrodes for Energy Applications," *ACS Appl. Energy Mater.*, vol. 3, no. 1, pp. 66–98, 2020, doi: 10.1021/acsaem.9b01965.
- [14] F. Ciucci, "Modeling electrochemical impedance spectroscopy," *Curr. Opin. Electrochem.*, vol. 13, pp. 132–139, 2019, doi: 10.1016/j.coelec.2018.12.003.
- [15] W. Choi, H. C. Shin, J. M. Kim, J. Y. Choi, and W. S. Yoon, "Modeling and applications of electrochemical impedance spectroscopy (Eis) for lithium-ion batteries," *J. Electrochem. Sci. Technol.*, vol. 11, no. 1, pp. 1–13, 2020, doi: 10.33961/jecst.2019.00528.
- [16] J. Kretzschmar and F. Harnisch, "Electrochemical impedance spectroscopy on biofilm electrodes – conclusive or euphonious?," *Curr. Opin. Electrochem.*, vol. 29, p. 100757, 2021, doi: 10.1016/j.coelec.2021.100757.
- [17] V. Balasubramani, S. Chandraleka, T. S. Rao, R. Sasikumar, M. R. Kuppusamy, and T. M. Sridhar, "Review – Recent Advances in Electrochemical Impedance Spectroscopy Based Toxic Gas Sensors Using Semiconducting Metal Oxides," *J. Electrochem. Soc.*, vol. 167, no. 3, p. 037572, 2020, doi: 10.1149/1945-7111/ab77a0.
- [18] J. R. Macdonald and W. B. Johnson, "Fundamentals of Impedance Spectroscopy 1.1 BACKGROUND, BASIC DEFINITIONS, AND HISTORY 1.1.1 The Importance of Interfaces," 2018.
- [19] S. Anantharaj and S. Noda, "Appropriate Use of Electrochemical Impedance Spectroscopy in Water Splitting Electrocatalysis," *ChemElectroChem*, vol. 7, no. 10, pp. 2297–2308, 2020, doi: 10.1002/celec.202000515.
- [20] T. Pajkossy and R. Jurczakowski, "Electrochemical impedance spectroscopy in interfacial studies," *Curr. Opin. Electrochem.*, vol. 1, no. 1, pp. 53–58, 2017, doi: 10.1016/j.coelec.2017.01.006.
- [21] L. A. Buscaglia, O. N. Oliveira, and J. P. Carmo, "Roadmap for Electrical Impedance Spectroscopy for Sensing: A Tutorial," *IEEE Sens. J.*, vol. 21, no. 20, pp. 22246–22257, 2021, doi: 10.1109/JSEN.2021.3085237.
- [22] N. O. Laschuk, E. B. Easton, and O. V. Zenkina, "Reducing the resistance for the use of electrochemical impedance spectroscopy analysis in materials chemistry," *RSC Adv.*,

- vol. 11, no. 45, pp. 27925–27936, 2021, doi: 10.1039/d1ra03785d.
- [23] M. Van Haeverbeke, M. Stock, and B. De Baets, “Equivalent Electrical Circuits and Their Use Across Electrochemical Impedance Spectroscopy Application Domains,” *IEEE Access*, vol. 10, pp. 51363–51379, 2022, doi: 10.1109/ACCESS.2022.3174067.
- [24] N. Meddings *et al.*, “Application of electrochemical impedance spectroscopy to commercial Li-ion cells: A review,” *J. Power Sources*, vol. 480, no. September, 2020, doi: 10.1016/j.jpowsour.2020.228742.
- [25] M. Esser, G. Rohde, and C. Rehtanz, “Electrochemical Impedance Spectroscopy Setup based on Standard Measurement Equipment,” *J. Power Sources*, vol. 544, 2022.
- [26] K. Almuhammadi, T. K. Bera, and G. Lubineau, “Electrical impedance spectroscopy for measuring the impedance response of carbon-fiber-reinforced polymer composite laminates,” *Compos. Struct.*, vol. 168, pp. 510–521, 2017, doi: 10.1016/j.compstruct.2017.02.075.
- [27] D. V. Ribeiro and J. C. C. Abrantes, “Application of electrochemical impedance spectroscopy (EIS) to monitor the corrosion of reinforced concrete: A new approach,” *Constr. Build. Mater.*, vol. 111, pp. 98–104, 2016, doi: 10.1016/j.conbuildmat.2016.02.047.
- [28] M. A. Zabara and B. Ulgut, “Electrochemical Impedance Spectroscopy based voltage modeling of lithium Thionyl Chloride (Li\SOCl<sub>2</sub>) primary battery at arbitrary discharge,” *Electrochim. Acta*, vol. 334, p. 135584, 2020, doi: 10.1016/j.electacta.2019.135584.
- [29] V. Sunil, B. Pal, I. Izwan Misnon, and R. Jose, “Characterization of supercapacitive charge storage device using electrochemical impedance spectroscopy,” *Mater. Today Proc.*, vol. 46, no. xxxx, pp. 1588–1594, 2020, doi: 10.1016/j.matpr.2020.07.248.
- [30] S. Wang, J. Zhang, O. Gharbi, V. Vivier, M. Gao, and M. E. Orazem, “Electrochemical impedance spectroscopy,” *Nat. Rev. Methods Prim.*, vol. 1, no. 1, 2021, doi: 10.1038/s43586-021-00039-w.
- [31] L. Fan and Z. Miao, “Admittance-Based Stability Analysis: Bode Plots, Nyquist Diagrams or Eigenvalue Analysis?,” *IEEE Trans. Power Syst.*, vol. 35, no. 4, pp. 3312–3315, 2020, doi: 10.1109/TPWRS.2020.2996014.
- [32] J. Huang, Z. Li, B. Y. Liaw, and J. Zhang, “Graphical analysis of electrochemical impedance spectroscopy data in Bode and Nyquist representations,” *J. Power Sources*, vol. 309, pp. 82–98, 2016, doi: 10.1016/j.jpowsour.2016.01.073.
- [33] H. H. Hernandez *et al.*, “Electrochemical Impedance Spectroscopy (EIS): A Review Study of Basic Aspect of the Corrosion Mechanism Applied to Steels,” *Books on Demand*, vol. 1, no. 1, p. 6, 2020, [Online]. Available: <http://dx.doi.org/10.5772/intechopen.87884>
- [34] M. Grossi and B. Riccò, “Electrical impedance spectroscopy (EIS) for biological analysis and food characterization: A review,” *J. Sensors Sens. Syst.*, vol. 6, no. 2, pp. 303–325, 2017, doi: 10.5194/jsss-6-303-2017.

- [35] Z. Lukács and T. Kristóf, "A generalized model of the equivalent circuits in the electrochemical impedance spectroscopy," *Electrochim. Acta*, vol. 363, 2020, doi: 10.1016/j.electacta.2020.137199.
- [36] G. Barbero and I. Lelidis, "Analysis of Warburg's impedance and its equivalent electric circuits," *Phys. Chem. Chem. Phys.*, vol. 19, no. 36, pp. 24934–24944, 2017, doi: 10.1039/c7cp04032f.
- [37] H. S. Magar, R. Y. A. Hassan, and A. Mulchandani, "Electrochemical impedance spectroscopy (Eis): Principles, construction, and biosensing applications," *Sensors*, vol. 21, no. 19, 2021, doi: 10.3390/s21196578.